On Annular Modes and Zonal Jets

ADAM H. MONAHAN

School of Earth and Ocean Sciences, University of Victoria, Victoria, British Columbia, and Earth System Evolution Program, Canadian Institute for Advanced Research, Toronto, Ontario, Canada

JOHN C. FYFE

Canadian Centre for Climate Modelling and Analysis, Meteorological Service of Canada, University of Victoria, Victoria, British Columbia, Canada

(Manuscript received 8 January 2007, in final form 11 June 2007)

ABSTRACT

This study considers the relation of the annular mode to the kinematics of a fluctuating jet in zonal-mean zonal wind and to the zonal index, using an idealized model of fluctuations in the eddy-driven jet. When the sphericity of the domain is accounted for, observed and numerically simulated annular modes for the Southern Hemisphere summertime are found to be in excellent agreement. In particular, the annular mode and zonal index mode are shown to be related but distinct. Although the annular mode is strongly (but not identically) related to fluctuations in jet position, fluctuations in jet strength and width are shown to also be important for its simulation. When the sphericity of the domain is neglected, analytic expressions for the leading empirical orthogonal function (EOF) modes of zonal-mean geopotential for the cases of individual fluctuations in jet strength, position, and width can be obtained. None of these EOF modes have the characteristics of the annular mode. In the presence of simultaneous fluctuations in jet strength and position, the leading zonal-mean geopotential EOF mode (strongly resembling the annular mode) is shown to mix the zonal index mode of zonal-mean zonal wind with other EOF modes, demonstrating why the annular mode and zonal index mode are related but distinct. The greater sensitivity to domain size of EOF modes of geopotential relative to the EOF modes of zonal-mean zonal wind is also discussed. This study focuses on the Southern Hemisphere summertime, which is characterized by a single, eddy-driven jet; the generality of the results presented suggest that the conclusions should be qualitatively unchanged in the presence of both subtropical and eddy-driven jets.

1. Introduction

Interest in the characteristic structures of zonal-mean variability of the circulation of the extratropical atmosphere extends at least as far back as the middle decades of the twentieth century (see Thompson et al. 2002, for a review). The dominant structure of variability in extratropical daily zonal-mean zonal wind in either hemisphere as obtained from empirical orthogonal function (EOF) analysis is found to be an equivalent barotropic dipole with oppositely signed anomalies in the low and high latitudes (the black curve in Fig. 1). The associated time series is denoted the zonal index, and together with the dipole spatial pattern is typically interpreted as describing fluctuations in the central latitude of the eddy-driven jet (e.g., Robinson 1996; Feldstein and Lee 1998; DeWeaver and Nigam 2000; Lorenz and Hartmann 2001; Codron 2005; Wittman et al. 2005). In this study, the zonal index time series and its associated spatial pattern in zonal-mean zonal wind will be referred to as the zonal index mode. The leading EOF of Northern Hemisphere (NH) extratropical sea level pressure (SLP) was defined by Thompson and Wallace (1998) as the Arctic Oscillation, or Northern Annular Mode [respectively the Antarctic Oscillation or Southern Annular Mode for the Southern Hemisphere (SH) SLP]. The EOF spatial structures are equivalent barotropic and dipole-like, and are approximately zonally symmetric with oppositely signed anomalies in the mid- and high latitudes. This zonal symmetry motivates consideration of the statistics of

Corresponding author address: Adam Monahan, School of Earth and Ocean Sciences, University of Victoria, P.O. Box 3055, STN CSC, Victoria, BC V8W 3P6, Canada.
E-mail: monahana@uvic.ca

DOI: 10.1175/2007JCLI1841.1

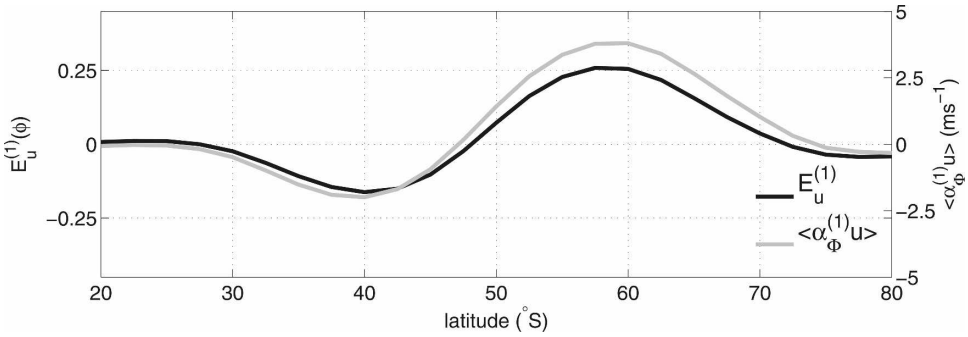

FIG. 1. Comparison of the zonal index mode and the annular mode from observations: leading EOF pattern of $E_u^{(1)}(\phi)$ of zonal-mean zonal wind (black line) and regression pattern of the leading zonal-mean geopotential PC time series $\alpha_\Phi^{(1)}(t)$ (standardized to unit variance) on the zonal-mean zonal wind (gray line). If the zonal index mode and the annular mode were interchangeable, the black and gray lines would coincide. The data used for these calculations were daily austral summer (December–January) SH 500-hPa geopotential height anomalies from 20° to 80°S taken from ERA-40 (available online at http://data.ecmwf.int/data/d/era40/).

the zonally averaged geopotential; the leading EOF of 500-hPa SH geopotential is shown in the black curve in the top panel of Fig. 2. We will denote this structure of variability as the annular mode, and it is interpreted as describing an exchange of mass between middle and high latitudes associated with an expansion or contraction of the polar vortex (e.g., Thompson and Wallace 2000; Thompson et al. 2002). Regressing the principal component (PC) time series corresponding to the annular mode on the zonal-mean zonal wind field yields a dipole pattern (the gray curve in Fig. 1), which is similar to the spatial structure of the zonal index mode and suggests a relationship between the annular mode and the eddy-driven jet. In consequence, the zonal index mode and the annular mode have often been treated as being more or less interchangeable.

In fact, the zonal index mode and the annular modes are not identical: in general, EOFs of physically related but distinct fields will not be related in a one-to-one fashion (e.g., Ambaum et al. 2001). A simple demonstration of this fact follows from consideration of a vector time series $\mathbf{X}$ (assumed to be of mean zero) arranged in a matrix such that the M stations correspond to the rows and the N observations correspond to the columns. This time series will have the singular value decomposition

$$\mathbf{X} = \mathbf{E}\mathbf{\Lambda}\mathbf{G}^{\mathrm{T}}, \tag{1}$$

where $\mathbf{E}$ is the $M \times M$ matrix of EOFs, $\mathbf{G}$ is the $N \times M$ array of PC time series (normalized to unit variance), and $\mathbf{\Lambda}$ is the $M \times M$ array of PC variances. The EOFs are the eigenvectors of the covariance matrix

$$\mathbf{C}_{\mathrm{XX}} = \mathbf{X}\mathbf{X}^{\mathrm{T}} = \mathbf{E}\mathbf{\Lambda}^2\mathbf{E}^{\mathrm{T}}, \tag{2}$$

and satisfy the orthogonality condition $\mathbf{E}\mathbf{E}^{\mathrm{T}} = \mathbf{I}$, where $\mathbf{I}$ is the $M \times M$ unit matrix. Another vector time series $\mathbf{Y}$ related to $\mathbf{X}$ through a linear transformation (such as the differential operator relating zonal-mean geopotential with zonal-mean zonal wind through the assumption of geostrophy)

$$\mathbf{Y} = \mathbf{D}\mathbf{X} = \mathbf{D}\mathbf{E}\mathbf{\Lambda}\mathbf{G}^{\mathrm{T}} \tag{3}$$

will have covariance matrix

$$\mathbf{C}_{\mathrm{YY}} = \mathbf{Y}\mathbf{Y}^{\mathrm{T}} = \mathbf{D}\mathbf{E}\mathbf{\Lambda}^2(\mathbf{D}\mathbf{E})^{\mathrm{T}}. \tag{4}$$

If the rows of $\mathbf{DE}$ are mutually orthogonal, then these will be parallel with the EOFs of $\mathbf{Y}$ and the EOFs of the transformed variable will be the transformed EOFs. In general, however, the rows of $\mathbf{DE}$ will not be orthogonal;

$$(\mathbf{D}\mathbf{E})(\mathbf{D}\mathbf{E})^{\mathrm{T}} = \mathbf{D}\mathbf{E}\mathbf{E}^{\mathrm{T}}\mathbf{D}^{\mathrm{T}} = \mathbf{D}\mathbf{D}^{\mathrm{T}}, \tag{5}$$

which is not generally diagonal. It follows that the EOFs of $\mathbf{Y}$ and the transformed EOFs of $\mathbf{X}$ do not generally coincide.

Inspection of Fig. 1 demonstrates that while the spatial patterns of both the zonal index mode and the regression of the annular mode on the zonal-mean zonal wind are asymmetric, with larger anomalies in high latitudes than in low latitudes, the degree of asymmetry is considerably stronger for the regression pattern. If the annular mode and the zonal index mode represented exactly the same aspect of variability, these two spatial structures would be identical. This difference in spatial structure reflects the fact that the zonal index mode and annular mode are not perfectly correlated: the correla-

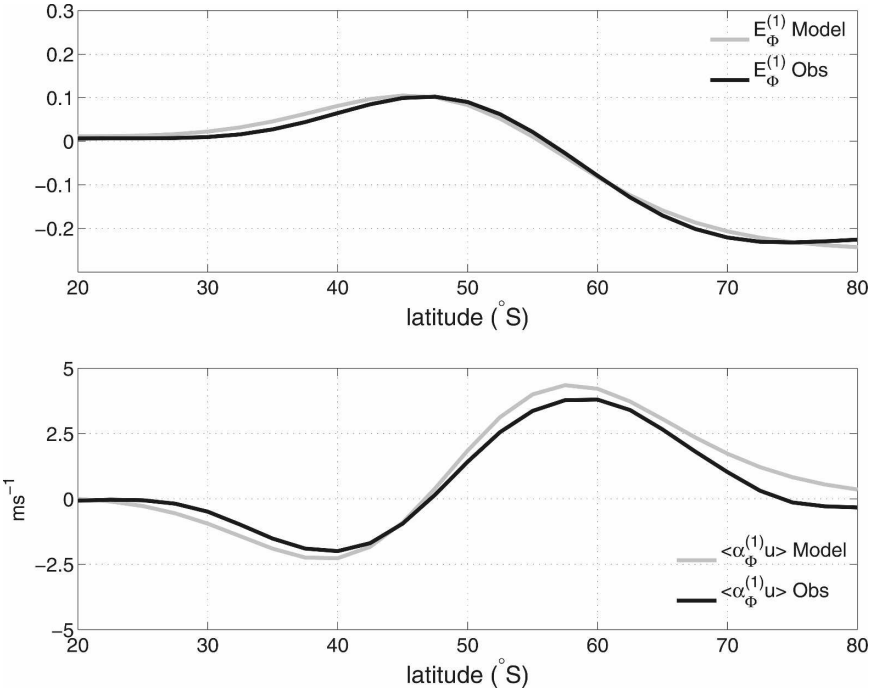

FIG. 2. (top) Leading geopotential height EOF $E_\Phi^{(1)}(\phi)$ and (bottom) regression patterns of zonal-mean zonal wind $u(\phi, t)$ on the PC time series of the leading geopotential EOF $\alpha_\Phi^{(1)}(t)$ (normalized to unit variance). The black lines correspond to observed austral summer SH variables and the gray lines are the simulated quantities with standard parameters.

tion coefficient between these two time series is 0.90 ± 0.02, which is high but not equal to 1. The confidence interval for the correlation was bootstrapped from an ensemble of five hundred 44-yr-long realizations drawn randomly (with replacement) from the observational data (described in the caption of Fig. 1); in any such realization, an average of 36% of years will be excluded. The zonal index mode and annular mode time series share 81% of their variance in common, with the implication that 19% of variability is *not* shared.

As was discussed in Wittman et al. (2005), the fact that the zonal index mode and the annular mode are robust features of observational data throughout the troposphere and a broad range of general circulation models (GCMs) of various degrees of complexity indicates that these statistical modes reflect some very generic aspect of midlatitude atmospheric variability. Using an idealized model of the extratropical eddy-driven jet in the zonal-mean wind, characterized by fluctuations in strength, position, and width, Fyfe and Lorenz (2005) and Wittman et al. (2005) demonstrated that fluctuations in jet position do indeed result in a dipolar EOF of zonal-mean zonal wind. Similarly, Vallis et al. (2004) considered the zonal-mean zonal wind EOFs resulting from quasigeostrophic, barotropic dynamics on a β plane subject to random "stirring" meant to represent the effect of baroclinic eddies. The resulting westerly jet displayed fluctuations in strength and position, the relative contribution of which depended primarily on the width of the stirring region. When fluctuations in jet position were dominant, the leading EOFs of zonal-mean zonal wind and of zonal-mean streamfunction resembled the spatial structures of the zonal index mode and annular mode, respectively. Gerber and Vallis (2005) used a simple stochastic model of zonal-mean zonal wind anomalies (with no assumptions made about the structure of the time-mean flow) to obtain analytic expressions for the EOFs. It was found that a dipole arises as the leading EOF of zonal-mean zonal wind in this idealized model if the anomalies conserve angular momentum and vanish at the northern and southern boundaries of the domain. Geopotential anomalies were then obtained through imposition of geostrophic balance and mass conservation; the leading EOF of the geopotential field was shown to be a monopole with a shifted baseline, with like-signed anomalies in high and low latitudes and oppositely signed anomalies in middle latitudes. This structure was suggestive of the annular mode, but was characterized by anomalies that were too weak in high latitudes and too strong in low latitudes.

The EOF structure of the zonal-mean zonal wind in

the idealized model of the fluctuating eddy-driven jet was analyzed in detail in Monahan and Fyfe (2006). The leading EOF structures produced by this model were in good agreement with the observed leading EOFs of observed austral wintertime SH 500-hPa geopotential zonal-mean zonal winds. Analytic expressions for the leading EOFs of the zonal-mean zonal wind and their associated time series were obtained through perturbation expansions of the covariance functions. It was shown that the EOFs are composed of linear combinations of monopole, dipole, and tripole patterns, such that individual EOF modes cannot generally be associated with individual jet fluctuation degrees of freedom (strength, position, or width). In particular, the zonal index mode in the model arises as a result of fluctuations in jet position, but the time series includes contributions from fluctuations in jet strength and width as well. It was concluded that no simple interpretation of individual zonal wind EOFs in terms of jet strength, position, or width fluctuations is possible in general.

The present study extends Monahan and Fyfe (2006) to consider the EOF structure of zonal-mean geopotential as obtained from the zonal-mean zonal wind through the assumptions of geostrophic balance and mass conservation, investigating the relationship between the annular mode and the kinematics of a fluctuating zonal jet. Most previous studies of the zonal index and the annular mode have first carried out an EOF analysis of either observed or simulated fields, and then interpreted the results in terms of jet variability. This study reverses the approach: the jet and its fluctuations will be prescribed, and the resulting EOF structures computed. It will be shown that the annular mode produced by the idealized model using jet parameters fit to observations is in excellent agreement with that from observations, particularly when sphericity of the domain is accounted for in the translation from zonal wind to geopotential. The modeled annular mode and zonal index mode are shown to be related but distinct, as suggested by Fig. 1. Analytic results for the EOF modes of zonal-mean geopotential are computed on a flat domain (neglecting effects of spherical geometry), allowing unambiguous diagnoses of the relationships between EOF modes and jet degrees of freedom (strength, position, and width). These computations also elucidate the reasons for the dependence of zonal-mean geopotential EOFs on the analysis domain and for the lack of a one-to-one correspondence between individual EOF modes of zonal-mean geopotential and zonal-mean zonal wind.

Because this study considers only zonally averaged fields, it does not touch on the debate considering the regional versus hemispheric nature of extratropical variability (i.e., the North Atlantic Oscillation versus the Northern Annular Mode; see Wallace 2000; Ambaum et al. 2001; Thompson et al. 2002; Cash et al. 2002; Kushner and Lee 2007). The focus on the extratropical SH allows the EOFs of zonally averaged quantities to be used interchangeably with the zonal averages of full hemispheric EOFs, because the two are essentially the same (Baldwin 2001). Furthermore, we will not address the physical mechanisms resulting in variability of the eddy-driven jet (e.g., Robinson 1996; Feldstein and Lee 1998; DeWeaver and Nigam 2000; Limpasuvan and Hartmann 2000; Lorenz and Hartmann 2001; Thompson et al. 2002; Vallis et al. 2004; Codron 2005); fluctuations in jet strength, position, and width will simply be prescribed. This simplification allows for a straightforward diagnosis of the relationship between EOF modes and the jet degrees of freedom.

The idealized fluctuating zonal jet model is presented in section 2. Section 3 presents numerically computed EOF modes of zonal-mean geopotential when the sphericity of the domain is taken into account. Analytic and numerical results for the EOFs of zonal-mean geopotential on a flat domain are presented in section 4. A discussion and conclusions are given in section 5.

2. The fluctuating Gaussian jet

Following previous studies (Fyfe 2003; Fyfe and Lorenz 2005; Wittman et al. 2005; Monahan and Fyfe 2006), we express variability in the zonal-mean zonal wind (on a specified pressure level) in terms of a jet that fluctuates in strength, position, and width,

$$u(\phi, t) = [U_0 + \xi(t)] \exp\left(-\frac{[\phi - \phi_0 - \lambda(t)]^2 [1 + \eta(t)]^2}{2\sigma_0^2} \right). \tag{6}$$

In Eq. (6), $\xi(t)$ and $\lambda(t)$ denote fluctuations in jet strength and central latitude, respectively. Following Monahan and Fyfe (2006), the quantity $\eta(t)$ denotes fluctuations in jet inverse width, scaled by the time-mean inverse width,

$$\sigma^{-1}(t) = \sigma_0^{-1}[1 + \eta(t)]. \tag{7}$$

Fluctuations in inverse jet width are considered because for the observed jets they are more closely Gaussian than are fluctuations in jet width. We further assume that $\xi(t)$, $\lambda(t)$, and $\eta(t)$ are individually Gaussian with mean 0 and respective standard deviations γ, w, and υ,

$$p(\xi) = \frac{1}{\sqrt{2\pi\gamma^2}} \exp\left(-\frac{\xi^2}{2\gamma^2}\right), \quad (8)$$

$$p(\lambda) = \frac{1}{\sqrt{2\pi w^2}} \exp\left(-\frac{\lambda^2}{2w^2}\right), \quad (9)$$

$$p(\eta) = \frac{1}{\sqrt{2\pi\upsilon^2}} \exp\left(-\frac{\eta^2}{2\upsilon^2}\right). \quad (10)$$

As was discussed in Monahan and Fyfe (2006), on short time scales the zonal-mean jet approximately conserves angular momentum, so $\xi(t)$ and $\eta(t)$ are positively correlated; as the jet widens (narrows), it must slow down (speed up). A correlation between jet strength and position that might be expected to follow from angular momentum conservation on a sphere is not observed when these parameters are estimated from observations, and it is therefore not included in the idealized model. Correlation between $\xi(t)$ and $\eta(t)$ is allowed for by setting

$$\xi(t) = \rho\eta(t) + (\gamma^2 - \rho^2\upsilon^2)^{1/2}\varepsilon(t), \quad (11)$$

where ρ is the covariance of $\xi(t)$ and $\eta(t)$, and $\varepsilon(t)$ is a Gaussian random process with mean zero and unit variance that is independent of $\eta(t)$ (reflecting observed deviations from perfect angular momentum conservation of winds at a single pressure level over a limited meridional range). Best-fit values of the jet parameters were estimated from daily austral summer (December–January) 500-hPa SH geopotential heights from 40-yr European Centre for Medium-Range Weather Forecasts (ECMWF) Re-Analysis (ERA-40; information available online at http://data.ecmwf.int/data/d/era40/) using the method described in Monahan and Fyfe (2006); these standard parameter values are listed in Table 1. Austral summertime data are considered because the subtropical jet is weak and so midlatitude variability is dominated by a single eddy-driven jet. In other seasons, variability is complicated by the presence of two fluctuating jets.

We now proceed to express the model of the fluctuating jet in terms of the geopotential. In geostrophic balance, the zonal-mean geopotential $\Phi(\phi, t)$ is related to the zonal-mean zonal wind $u(\phi, t)$ through the integral

$$\Phi(\phi, t) = -\int_{\phi_1}^{\phi} f(\phi')u(\phi', t)\, d\phi' + c(t), \quad (12)$$

where $\mathcal{D} = (\phi_1, \phi_2)$ is the domain under consideration, $f(\phi)$ is the Coriolis parameter, and $c(t)$ is a (time dependent) constant of integration. Thus defined, $\Phi(\phi, t)$ differs from the true geopotential by a multiplicative constant (for ϕ in radians, this constant is one over the radius of the earth). Such multiplicative constants have no effect on the EOF structure of the field, and so will be neglected in subsequent calculations. Throughout this study, the analysis domain will be $\mathcal{D} = (20°\text{S}, 80°\text{S})$ (the results are qualitatively unchanged if the poleward limit of the domain is taken to the South Pole).

TABLE 1. Standard austral summertime SH 500-hPa zonal-mean zonal jet parameters; estimated as described in Monahan and Fyfe (2006).

Quantity	Symbol	Standard value
Time-mean jet central latitude	ϕ_0	47.5°
Standard deviation of jet position fluctuations	w	3.26°
Time-mean jet strength	U_0	23.3 m s^{-1}
Standard deviation in jet strength	γ	2.6 m s^{-1}
Time-mean jet width	σ_0	9.6°
Standard deviation in inverse-scaled jet width	υ	0.18
Covariance of strength and inverse-scaled jet width	ρ	10.3 m s^{-1}

As noted in Gerber and Vallis (2005), the constant of integration in Eq. (12) can be specified by assuming that variability in the jet conserves mass below the specified isobaric surface. In the absence of temperature fluctuations below the pressure level at which the geopotential is specified, an increase (say) in Φ at high latitudes implies a local increase in surface pressure and thus a local increase in the mass of the atmospheric column. This mass must come from elsewhere; in the zonal average in can only come from lower latitudes, so there must be a decrease in Φ at these latitudes. Temperature changes below the pressure level under consideration can change the distribution of geopotential without changing that of mass: in hydrostatic equilibrium, warming (cooling) of the atmospheric column produces an increase (decrease) of the altitude separation of pressure surfaces. While such thermally driven changes in geopotential are expected to be significant over long time scales (such at those associated with anthropogenic climate change), they are not expected to be of leading-order importance on daily to weekly time scales in the presence of a vigorously fluctuating eddy-driven jet.

The mass below the specified pressure surface is proportional to the quantity $M(t)$, defined as

$$M(t) = \frac{1}{g}\{\Phi(\phi, t)\} - \{H(\phi)\}, \quad (13)$$

where g is the acceleration of gravity, $H(\phi)$ is the zonally integrated topographic elevation, and the brackets denote the weighted average

$$\{h(\phi)\} = \int_{\phi_1}^{\phi_2} \mu(\phi) h(\phi)\, d\phi, \tag{14}$$

where $\mu(\phi)$ is a latitudinally dependent weighting function defined so that

$$\int_{\phi_1}^{\phi_2} \mu(\phi)\, d\phi = 1. \tag{15}$$

Mass conservation is ensured by requiring that $\{\Phi(\phi)\}$ is constant; without loss of generality, we take $\{\Phi(\phi)\} = 0$:

$$\Phi(\phi, t) = -\int_{\phi_1}^{\phi} f(\phi') u(\phi', t)\, d\phi' + \left\{ \int_{\phi_1}^{\phi} f(\phi') u(\phi', t)\, d\phi' \right\}. \tag{16}$$

To assess the extent to which $M(t)$ is conserved in observations, this quantity was calculated over the standard domain $\mathcal{D}$ for daily austral summer (December–January) SH zonal-mean 500-hPa ERA-40 geopotential heights. It was found that the standard deviation of $M(t)$ was 1% of the mean value; hence, $M(t)$ is conserved to an excellent approximation in these data.

3. Spherical domain

We first consider the EOFs of geopotential on a spherical domain, for which $f(\phi) = \sin\phi$ and

$$\mu(\phi) = \frac{\cos\phi}{\sin\phi_2 - \sin\phi_1}. \tag{17}$$

An overview of EOF analysis and the associated notation used in this study is given in the appendix. An effect of the sphericity of the domain is to amplify the variance of $\Phi(\phi, t)$ at high latitudes and to attenuate it at low latitudes. There are two reasons for this: first, the latitude dependence of the Coriolis parameter $f(\phi)$ implies that a unit fluctuation in zonal-mean zonal wind implies a larger fluctuation in geopotential at higher than at lower latitudes. Second, the $\cos(\phi)$ weighting of the mass conservation constraint implies that a unit change in Φ at low latitudes requires a larger change in Φ at higher latitudes to ensure that $\{\Phi(\phi)\} = 0$. Together, these aspects of working on a spherical domain tend to amplify the EOF pattern anomalies toward higher latitudes and attenuate them toward lower latitudes.

It is not clear how to obtain analytic solutions for the EOF structure of $\Phi(\phi, t)$ on the spherical domain; results are therefore obtained numerically. The leading EOF pattern of $\Phi(\phi, t)$ simulated on the spherical domain using the standard jet parameters (Table 1) is displayed in the upper panel of Fig. 2, along with $E_\Phi^{(1)}(\phi)$ from observed austral summer (December–January) SH geopotential heights. The agreement between the simulated and observed leading EOF spatial structures is striking: the relative amplitudes of the low- and high-latitude anomalies and the latitude of the zero crossing are all well simulated. The idealized model does an excellent job in reproducing the observed annular mode.

The lower panel of Fig. 2 illustrates the regression coefficients (both observed and simulated) between the zonal-mean zonal wind and the leading geopotential PC $\alpha_\Phi^{(1)}(t)$ (normalized to unit variance). The dipolar structure of the regression pattern in observations, with smaller values in the lower than in the higher latitudes and a zero crossing near the mean jet axis, is captured well in the simulated regression pattern (although the simulated lower-latitude maximum and higher-latitude minimum are slightly overestimated).

Despite the similarity of the regression pattern between $u(\phi, t)$ and $\alpha_\Phi^{(1)}(t)$ to the zonal index mode spatial pattern $E_u^{(1)}(\phi)$ (e.g., Monahan and Fyfe 2006), there is not a one-to-one correspondence between the leading EOFs of geopotential and zonal-mean zonal wind. As discussed previously, the low- and high-latitude extrema of the zonal index mode spatial pattern are closer in amplitude than are the low- and high-latitude extrema of the regression patterns, for which the high-latitude lobe is considerably larger. Furthermore, observed and simulated correlation coefficients between $\alpha_\Phi^{(1)}(t)$ and $\alpha_u^{(1)}(t)$ are, respectively, 0.90 and 0.78. In neither observations nor simulations is the variability characterized by the annular mode identical to that of the zonal index mode.

A useful feature of the fluctuating zonal jet model is that the relation of the simulated PC time series to the fluctuations in strength, position, and width can be directly investigated. The correlation coefficient of the annular mode time series $\alpha_\Phi^{(1)}(t)$ with the jet position anomaly $\lambda(t)$ is 0.80 in observations and 0.85 in the model. Correlations of $\alpha_\Phi^{(1)}(t)$ with jet strength and inverse width fluctuations [$\xi(t)$ and $\eta(t)$, respectively] are weak both in the model (respectively, 0.08 and -0.31) and in the observations (respectively, -0.21 and 0.00). Although the correlations between the annular mode and jet position are strong, to the extent that these correlations are not perfect, the annular mode does not simply describe fluctuations in jet position.

A further benefit of the fluctuating zonal jet model is that the covariance structure associated with pure fluctuations in each of strength, position, and width individually can be investigated (as in Wittman et al. 2005; Monahan and Fyfe 2006). The leading EOF patterns

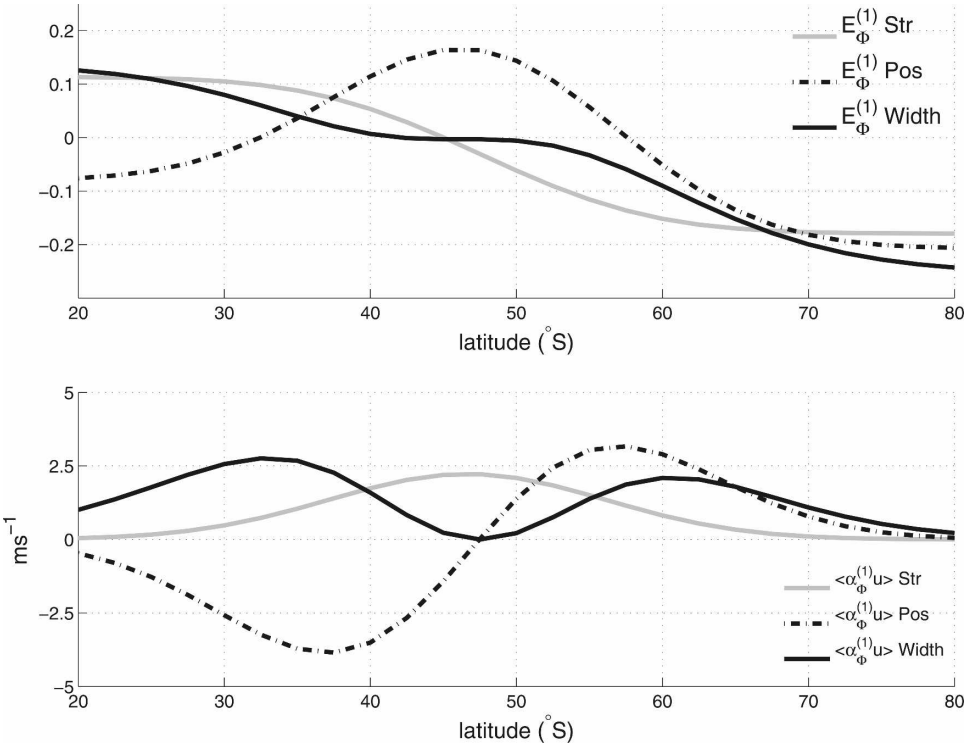

FIG. 3. (top) Leading geopotential EOFs $E_\Phi^{(1)}(\phi)$ on the spherical domain for fluctuations in strength alone (solid gray line), position alone (dot–dash line), and width alone (solid black line); and (bottom) plots of regression coefficients of zonal-mean zonal wind on the leading PC of geopotential $\alpha_\Phi^{(1)}(t)$ for fluctuations in strength alone (solid gray line), position alone (dot–dash line), and width alone (solid black line).

$E_\Phi^{(1)}(\phi)$ for each of these cases are illustrated in the upper panel of Fig. 3. Of the leading EOF structures associated with each of these special cases, that of fluctuations in jet position alone most resembles the observed leading EOF in $\Phi(\phi, t)$, although even here the agreement is poor (the midlatitude maximum is too large, and the pattern has a low-latitude zero crossing not present in the observed annular mode; see Fig. 1). The regression patterns of $\alpha_\Phi^{(1)}(u)$ on $u(\phi, t)$ for the cases of pure fluctuations in strength, position, and width are, respectively, monopolar, dipolar, and tripolar, strongly suggestive of the leading EOFs of zonal-mean zonal wind computed in Monahan and Fyfe (2006) for each of these special cases. A clear one-to-one correspondence between the leading EOFs of zonal-mean geopotential and zonal-mean zonal wind, absent in the presence of simultaneous fluctuations in jet strength, position, and width, is evident when each of these is present individually.

In the presence of fluctuations in both strength and position, but with no fluctuations in width, the leading EOF of zonal-mean geopotential bears a strong resemblance to the observed annular mode (black line in upper panel of Fig. 4). Similarly, the regression of zonal-mean zonal wind on $\alpha_\Phi^{(1)}(t)$ (black curve in lower panel of Fig. 4) strongly resembles the observed regression pattern, with stronger anomalies in the high than in the low latitudes.

We see that a strikingly good representation of the annular mode and its relationship to the zonal-mean zonal wind can be obtained from the idealized zonal jet model on a spherical domain, but only when fluctuations other than jet position are accounted for. Even though correlations of the annular mode with fluctuations in jet strength and width are weak, these jet degrees of freedom are needed for its accurate simulation. Unfortunately, the development of analytic expressions for the EOF spatial structures and PC time series of $u(\phi, t)$ (as in Monahan and Fyfe 2006) is not straightforward on a spherical domain. Such analytic results for the EOF modes of $\Phi(\phi, t)$ can be obtained if the sphericity of the domain is neglected, as is discussed in the following section.

4. Flat domain

Monahan and Fyfe (2006) derived analytic expressions for the EOFs and PCs of zonal-mean zonal wind

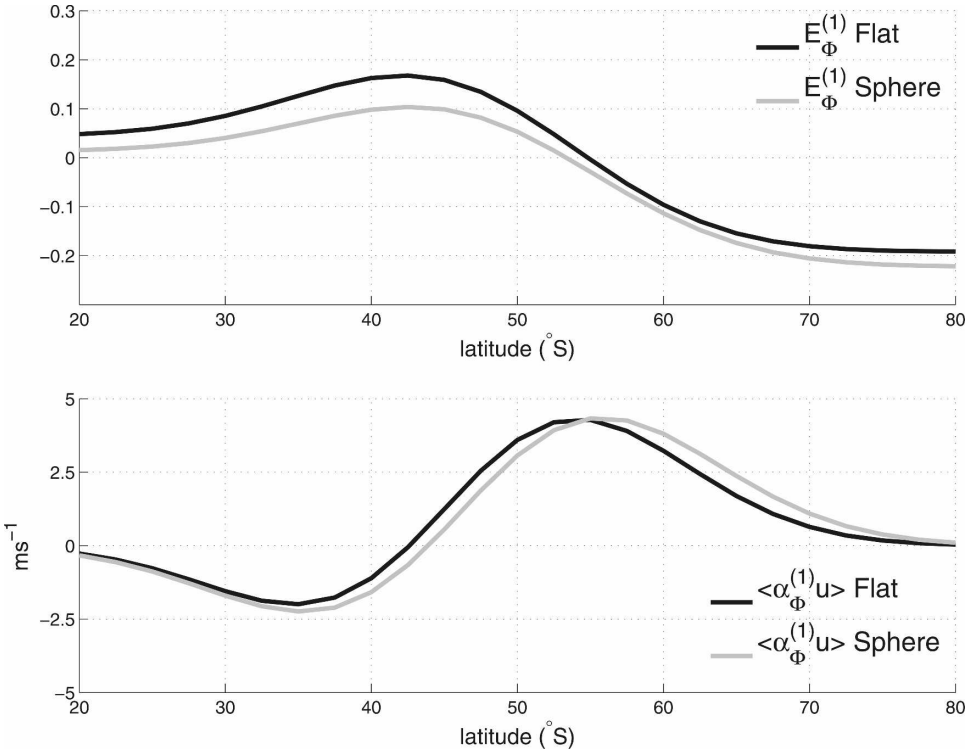

FIG. 4. The case of independent fluctuations in strength and position: (top) leading geopotential EOF $E_\Phi^{(1)}(\phi)$ on a flat domain (black line) and on a spherical domain (gray line) and (bottom) regression of $u(\phi, t)$ on $\alpha_\Phi^{(1)}(t)$ on a flat domain (black line) and on a spherical domain (gray line).

for the idealized zonal jet model in the cases of fluctuations in jet position, strength, and width individually, and of fluctuations in both jet position and strength together. In this section, we use the results of this earlier study to compute analytic expressions for the EOFs and PCs of zonal-mean geopotential for these illustrative limiting cases.

If we neglect the sphericity of the earth, $f(\phi)$ is a constant (which we can take without loss of generality to be one) and

$$\mu(\phi) = \frac{1}{\phi_2 - \phi_1}. \tag{18}$$

As is discussed in the appendix, the wind field can be expanded over its EOF basis

$$u(\phi, t) - \langle u(\phi)\rangle = \sum_{j=1}^{J} \alpha_u^{(j)}(t) E_u^{(j)}(\phi); \tag{19}$$

thus, assuming geostrophy and mass conservation,

$$\Phi(\phi, t) - \langle \Phi(\phi)\rangle = -\sum_{j=1}^{J} N_j \alpha_u^{(j)}(t) F_j(\phi), \tag{20}$$

where the functions

$$F_j(\phi) = \frac{1}{N_j}\left(\int_{\phi_1}^{\phi} E_u^{(j)}(\phi')\, d\phi' - \left\{ \int_{\phi_1}^{\phi} E_u^{(j)}(\phi')\, d\phi' \right\} \right) \tag{21}$$

are normalized to have unit L^2 norm [i.e., $\int_{\phi_1}^{\phi_2} F_j^2(\phi) d\phi = 1$] by taking

$$N_j = \left[\int_{\phi_1}^{\phi_2} \left(\int_{\phi_1}^{\phi} E_u^{(j)}(\phi')\, d\phi' - \left\{ \int_{\phi_1}^{\phi} E_u^{(j)}(\phi')\, d\phi' \right\} \right)^2 d\phi \right]^{1/2}. \tag{22}$$

The time series $\alpha_u^{(j)}(t)$ are all mutually uncorrelated, so the normalized functions $F_j(\phi)$ will correspond to EOFs $E_\Phi^{(j)}(\phi)$ of $\Phi(\phi, t)$ if they form an orthonormal set (because EOFs are orthogonal by definition). In fact, these functions will not be mutually orthogonal in general. The inner product of $F_j(\phi)$ and $F_k(\phi)$ is given by

$$\int_{\phi_1}^{\phi_2} F_j(\phi)F_k(\phi)\,d\phi = \frac{1}{N_jN_k}\int_{\phi_1}^{\phi_2}\left(\int_{\phi_1}^{\phi} E_u^{(j)}(\phi')\,d\phi'\right)\left(\int_{\phi_1}^{\phi} E_u^{(k)}(\phi'')\,d\phi''\right)d\phi - \frac{(\phi_2-\phi_1)}{N_jN_k}\left\{\int_{\phi_1}^{\phi} E_u^{(j)}(\phi')\,d\phi'\right\}\left\{\int_{\phi_1}^{\phi} E_u^{(k)}(\phi')\,d\phi'\right\}. \quad (23)$$

This inner product will not generally vanish because

1) the integrated functions $\int_{\phi_1}^{\phi} E_u^{(j)}(\phi')d\phi'$ will not, in general, be mutually orthogonal, and
2) the mass-weighted averages $\{\int_{\phi_1}^{\phi} E_u^{(j)}(\phi')d\phi'\}$ will generally be nonzero.

As was discussed in more general terms in section 1, a one-to-one relationship between EOF modes of geopotential and those of zonal-mean wind cannot be expected to hold in general. In particular, the EOF structure of geopotential is expected to be more sensitive to the analysis domain $\mathcal{D} = (\phi_1, \phi_2)$ than is the case for the EOF structure of the zonal wind. Equation (23) demonstrates that this domain dependence arises in two distinct ways—through the mass-weighted averages $\{\int_{\phi_1}^{\phi} E_u^{(j)}(\phi')d\phi'\}$ and through the normalizations N_j [Eq. (22)].

We now proceed to consider the EOF structure of the zonal-mean geopotential on the flat domain for the cases of pure fluctuations in jet strength, position, and width alone, and for independent fluctuations in jet strength and position. The basis functions $f_j(\phi)$ from which the EOF patterns of $u(\phi, t)$ were constructed in Monahan and Fyfe (2006), and which are used extensively below, are described in detail in the appendix.

a. Fluctuations in jet strength alone

As was shown in Monahan and Fyfe (2006), when the jet fluctuates in strength alone the zonal wind has only a single nontrivial EOF: the monopole $f_0(\phi)$ [the gravest of the set of orthogonal functions $f_j(\phi)$ defined in Eq. (A5)]. Thus, we may write

$$u(\phi, t) - \langle u(\phi)\rangle = (\sqrt{\pi}\sigma_0)^{1/2}\xi(t)f_0(\phi). \quad (24)$$

It follows that (using the results of the appendix)

$$\Phi(\phi, t) - \langle\Phi(\phi)\rangle = -\sqrt{2}\sigma_0\xi(t)\left[\operatorname{erf}\left(\frac{\phi-\phi_0}{\sqrt{2}\sigma_0}\right) - \left\{\operatorname{erf}\left(\frac{\phi-\phi_0}{\sqrt{2}\sigma_0}\right)\right\}\right]. \quad (25)$$

For the case of fluctuations in jet strength alone, the geopotential also has a single nontrivial EOF, with a spatial structure corresponding to an error function with a shifted baseline (illustrated in Fig. 5). This EOF structure has oppositely signed anomalies on either sign of the mean jet axis, and is associated with a meridional exchange of mass; in this sense, it is reminiscent of the annular mode. However, in contrast with the annular mode, the low-latitude anomaly amplitudes are approximately the same magnitude as the high-latitude anomaly amplitudes.

The regression of $u(\phi, t)$ on $\alpha_\Phi^{(1)}(t)$ (normalized to unit variance) is given by

$$\left\langle (u(\phi, t) - \langle u(\phi)\rangle)\left(\frac{\alpha_\Phi^{(1)}(t)}{\operatorname{std}(\alpha_\Phi^{(1)})}\right)\right\rangle = (\sqrt{\pi}\sigma_0)^{1/2}\gamma f_0(\phi). \quad (26)$$

This regression pattern, plotted in the lower panel of Fig. 5, is a monopole like the corresponding regression pattern on a spherical domain (Fig. 3) and the leading EOF of $u(\phi, t)$ for this special case. This latter result is a simple consequence of the one-to-one correspondence between the leading EOFs of zonal-mean zonal wind and zonal-mean geopotential for this special case.

b. Fluctuations in jet position alone

Monahan and Fyfe (2006) showed that in the limit that fluctuations in jet position are much smaller than the mean jet width ($h^2 = w^2/\sigma_0^2 \ll 1$, a limit relevant to the observed tropospheric jets), the leading two EOFs of a jet fluctuating in position alone are the dipole $f_1(\phi)$ and the tripole $f_2(\phi)$,

$$u(\phi, t) - \langle u(\phi)\rangle = \left(\frac{\sqrt{\pi}}{2\sigma_0}\right)^{1/2} U_0\left[\lambda(t)f_1(\phi) + \frac{\sqrt{6}}{4\sigma_0}(\lambda^2(t) - w^2)f_2(\phi)\right] + O(h^3), \quad (27)$$

so $\operatorname{var}(\alpha_u^{(1)}) \sim h^2$ and $\operatorname{var}(\alpha_u^{(2)}) \sim h^4$. Using the results of the appendix, it follows that

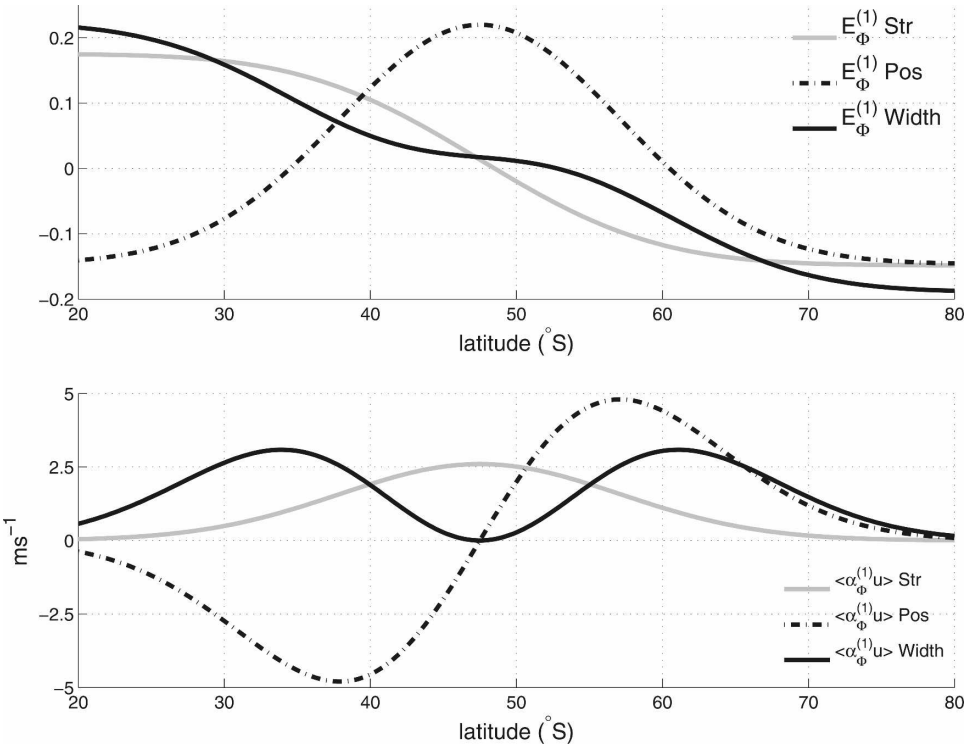

FIG. 5. As in Fig. 3, but on the flat domain.

$$\Phi(\phi, t) - \langle\Phi(\phi)\rangle = (\sqrt{\pi}\sigma_0)^{1/2} U_0 \left(N_1 \lambda(t) \frac{[f_0(\phi) - \{f_0(\phi)\}]}{N_1} + \frac{\sqrt{2}}{4\sigma_0} [\lambda^2(t) - w^2] f_1(\phi) \right) + O(h^3), \tag{28}$$

where we have used the results of the appendix and the fact that (to a good approximation) $\{f_1(\phi)\} \simeq 0$. For the standard parameter values, $N_1 = 0.66$. The time series $a_u^{(1)}(t)$ and $a_u^{(2)}(t)$ are uncorrelated (by construction), and $(f_0(\phi) - \{f_0(\phi)\})/N_1$ and $f_1(\phi)$ are normalized and orthogonal (by symmetry), so these functions are the leading two EOFs of zonal-mean geopotential. As was the case with fluctuations in jet strength alone, in the presence of fluctuations in jet position alone the EOFs of $u(\phi, t)$ are in a one-to-one correspondence with the EOFs of $\Phi(\phi, t)$, with time series that are identical, except that the standard deviation of $\alpha^{(1)}(t)$ relative to the standard deviation of $\alpha^{(2)}(t)$ is a factor of $\sqrt{3}N_1 = 1.15$ greater for geopotential height than for zonal winds. Not surprisingly, more variance is concentrated on larger spatial scales in the geopotential height field than in the zonal wind field; this transfer of variance to larger spatial scales increases with the size of the domain. As the domain becomes much wider than the mean jet, $N_1 \to 1$ and the amplification factor approaches $\sqrt{3}$.

The spatial structure of $E_\Phi^{(1)}(\phi)$ is given in the upper panel of Fig. 5. Like the annular mode, it is characterized by oppositely signed anomalies in the middle and high latitudes. However, in contrast to the annular mode, this structure has strong anomalies in low latitudes (like signed with those in high latitudes), and the middle- and high-latitude anomalies are of roughly the same size. While this pattern is reminiscent of the annular mode, the two are clearly distinct.

The regression of $u(\phi, t)$ on $\alpha_\Phi^{(1)}(t)$ (normalized to unit variance) is given by

$$\left\langle (u(\phi, t) - \langle u(\phi)\rangle) \left(\frac{\alpha_\Phi^{(1)}(t)}{\mathrm{std}(\alpha_\Phi^{(1)})} \right) \right\rangle = \left(\frac{\sqrt{\pi}}{2\sigma_0} \right)^{1/2} U_0 w f_1(\phi). \tag{29}$$

This regression pattern, plotted in the lower panel of Fig. 5, is a symmetric dipole like the corresponding regression pattern on a spherical domain (Fig. 3) and the leading EOF of $u(\phi, t)$ in this special case. This latter result is a simple consequence of the one-to-one correspondence between the leading EOFs of zonal-mean zonal wind and zonal-mean geopotential in this special case.

c. Fluctuations in jet width alone

It was shown in Monahan and Fyfe (2006) that in the limit that fluctuations in jet width are much smaller than the jet width itself ($v^2 \ll 1$), the leading EOF is a mixture of the monopole and tripole, so

$$u(\phi, t) - \langle u(\phi)\rangle = \left(\frac{3\sqrt{\pi}\sigma_0}{4}\right)^{1/2} U_0 \eta(t)\left(f_2(\phi) + \frac{2}{\sqrt{3}} f_0(\phi)\right) + O(v). \tag{30}$$

It follows from the results of the appendix that

$$\Phi(\phi, t) - \langle \Phi(\phi)\rangle = \left(\frac{\sqrt{\pi}\sigma_0^3}{2}\right)^{1/2} U_0 \eta(t)\left(f_1(\phi) - \frac{2}{(\sigma_0\sqrt{\pi})^{1/2}}\left[\operatorname{erf}\left(\frac{\phi - \phi_0}{\sqrt{2}\sigma_0}\right) - \left\{\operatorname{erf}\left(\frac{\phi - \phi_0}{\sqrt{2}\sigma_0}\right)\right\}\right]\right) + O(v), \tag{31}$$

and thus

$$E_\Phi^{(1)}(\phi) = \frac{1}{N_1}\left(f_1(\phi) - \frac{2}{(\sigma_0\sqrt{\pi})^{1/2}}\left[\operatorname{erf}\left(\frac{\phi - \phi_0}{\sqrt{2}\sigma_0}\right) - \left\{\operatorname{erf}\left(\frac{\phi - \phi_0}{\sqrt{2}\sigma_0}\right)\right\}\right]\right) \tag{32}$$

is the leading EOF of zonal-mean geopotential for the case of pure fluctuations in jet width. This structure (illustrated in Fig. 5) has oppositely signed anomalies on either side of the jet central latitude, like the leading EOF structure in the case of fluctuations of strength alone and the observed annular mode. Otherwise, it bears very little resemblance to the observed annular mode.

The regression of $u(\phi, t)$ on $\alpha_\Phi^{(1)}(t)$ (normalized to unit variance) is given by

$$\left\langle (u(\phi, t) - \langle u(\phi)\rangle)\left(\frac{\alpha_\Phi^{(1)}}{\operatorname{std}(\alpha_\Phi^{(1)})}\right)\right\rangle = \left(\frac{3\sqrt{\pi}\sigma_0}{4}\right)^{1/2} U_0 v\left(f_2(\phi) + \frac{2}{\sqrt{3}} f_0(\phi)\right). \tag{33}$$

This regression pattern, plotted in the lower panel of Fig. 5, is a tripole like the corresponding regression pattern on a spherical domain (Fig. 3) and the leading EOF of $u(\phi, t)$ in this special case. This latter result is a simple consequence of the one-to-one correspondence between the leading EOFs of zonal-mean zonal wind and zonal-mean geopotential in this special case.

d. Independent fluctuations in jet strength and position

For the case in which the jet displays independent fluctuations in both position and strength, in the $h^2 \ll 1$ limit, Monahan and Fyfe (2006) demonstrated that the leading EOFs are $\{f_1(\phi), E_u^{(+)}(\phi), E_u^{(-)}(\phi)\}$, where $E_u^{(+)}(\phi)$ and $E_u^{(-)}(\phi)$ are normalized and mutually orthogonal monopole–tripole hybrid functions

$$E_u^{(\pm)}(\phi) = \beta_0^{(\pm)} f_0(\phi) + \beta_2^{(\pm)} f_2(\phi). \tag{34}$$

Thus,

$$u(\phi, t) - \langle u(\phi)\rangle = \alpha_u^{(1)}(t) f_1(\phi) + \alpha_u^{(+)}(t) E_u^{(+)}(\phi) + \alpha_u^{(-)} E_u^{(-)}(\phi) + \text{h.o.t.} \tag{35}$$

The PC time series have variances

$$\operatorname{var}(\alpha_u^{(1)}) = \frac{\sqrt{\pi}\sigma_0 U_0^2}{2} h^2, \tag{36}$$

$$\operatorname{var}(\alpha_u^{(+)}) = \frac{\sqrt{\pi}\sigma_0 U_0^2}{2} l^2\left(1 + \delta + \sqrt{(1+\delta)^2 - \frac{8}{3}\delta}\right), \tag{37}$$

$$\operatorname{var}(\alpha_u^{(-)}) = \frac{\sqrt{\pi}\sigma_0 U_0^2}{2} l^2\left(1 + \delta - \sqrt{(1+\delta)^2 - \frac{8}{3}\delta}\right), \tag{38}$$

where

$$l = \frac{\gamma}{U_0} \tag{39}$$

and

$$\delta = \frac{3h^4}{8l^2}. \tag{40}$$

The coefficients $\beta_0^{(\pm)}$ and $\beta_2^{(\pm)}$ depend on the relative magnitudes of fluctuations in jet strength and jet position,

$$\beta_0^{(\pm)} = \frac{l^2}{\sqrt{3}[l^2 - \mathrm{var}(\alpha_u^{(\pm)})/(\sqrt{\pi}\sigma_0 U_0^2)]}\beta_2^{(\pm)}, \quad (41)$$

with normalization constraint

$$(\beta_0^{(\pm)})^2 - \frac{2}{\sqrt{3}}\beta_0^{(\pm)}\beta_2^{(\pm)} + (\beta_2^{(\pm)})^2 = 1. \quad (42)$$

The ordering of the EOFs depends on the relative sizes of l and h; the dipole $f_1(\phi)$ will be the leading EOF if $\mathrm{var}(\alpha_u^{(1)})/\mathrm{var}(\alpha_u^{(+)}) > 1$, and the hybrid monopole/tripole EOF $E_u^{(+)}(\phi)$ will be the leading EOF if $\mathrm{var}(\alpha_u^{(1)})/\mathrm{var}(\alpha_u^{(+)}) < 1$. For the standard parameters, $\delta = 0.4$, $\mathrm{var}(\alpha_u^{(1)})/\mathrm{var}(\alpha_u^{(+)}) = 3.9$ and the dipole is the leading EOF of u, so we can write

$$u(\phi, t) - \langle u(\phi)\rangle = \alpha_u^{(1)}(t)f_1(\phi) + \alpha_u^{(2)}(t)E_u^{(+)}(\phi) + \alpha_u^{(3)}E_u^{(-)}(\phi) + \text{h.o.t.} \quad (43)$$

For the standard parameters, $\mathrm{var}[\alpha_u^{(3)}(t)] \ll \mathrm{var}[\alpha_u^{(2)}(t)]$, and so it follows from the results of the appendix that to a good approximation,

$$\Phi(\phi, t) - \langle\Phi(\phi)\rangle \simeq b_1(t)F_1(\phi) + b_2(t)F_2(\phi), \quad (44)$$

where

$$F_1(\phi) = -\sqrt{2}\sigma_0\frac{[f_0(\phi) - \{f_0(\phi)\}]}{N_1}, \quad (45)$$

$$F_2(\phi) = \frac{1}{N_2}\left(\beta_0^{(+)}\left(\frac{2\sigma_0}{\sqrt{\pi}}\right)^{1/2}\left[\mathrm{erf}\left(\frac{\phi - \phi_0}{\sqrt{2}\sigma_0}\right) - \left\{\mathrm{erf}\left(\frac{\phi - \phi_0}{\sqrt{2}\sigma_0}\right)\right\}\right] - \beta_2^{(+)}\sqrt{\frac{2}{3}}\sigma_0 f_1(\phi)\right), \quad (46)$$

$$b_1(t) = -N_1\left(\frac{\sqrt{\pi}}{2\sigma_0}\right)^{1/2}(U_0 + \xi(t))\lambda(t), \quad (47)$$

$$b_2(t) = -N_2\left[\beta_0^{(+)}(\sqrt{\pi}\sigma_0)^{1/2}\left(\xi(t) - \frac{U_0}{4\sigma_0^2}(\lambda^2(t) - w^2) - \frac{\lambda^2(t)\xi(t)}{4\sigma_0^2}\right) + \beta_2^{(+)}\left(\frac{3\sqrt{\pi}}{\sigma_0}\right)^{1/2}\frac{(U_0 + \xi(t))}{4\sigma_0}(\lambda(t)^2 w^2)\right] \quad (48)$$

[using the expressions for $\alpha_u^{(1)}(t)$ and $\alpha_u^{(2)}(t)$ from Monahan and Fyfe (2006)]. For standard parameter values, $\beta_0 = -0.83$, $\beta_2 = 0.25$, $N_1 = 9.2$, and $N_2 = 18.9$. Note that as the domain size increases, $N_1 \to \sqrt{2}\sigma_0$ and $N_2 \propto \sqrt{\phi_2 - \phi_1}$; because the error function is not localized, its norm grows with domain size. In general, the functions $F_1(\phi)$ and $F_2(\phi)$ will not be orthogonal, and the leading EOFs of $\Phi(\phi, t)$ will be hybrids of these two structures,

$$E_\Phi^{(j)}(\phi) = a_1^{(j)}F_1(\phi) + a_2^j F_2(\phi). \quad (49)$$

For the standard parameter values, the spatial correlation coefficient of these two functions is

$$I = \int_{\phi_1}^{\phi_2} F_1(\phi)F_2(\phi)\,d\phi = -0.1. \quad (50)$$

Because $b_1(t)$ and $b_2(t)$ are uncorrelated, the zonal-mean geopotential covariance function is

$$C_{\Phi\Phi}(\phi', \phi'') = \langle b_1^2\rangle F_1(\phi')F_1(\phi'') + \langle b_2^2\rangle F_2(\phi')F_2(\phi''), \quad (51)$$

and thus the integral equation for the EOFs can be expressed as the 2×2 eigenvalue problem

$$\begin{pmatrix} \langle b_1^2\rangle & \langle b_1^2\rangle I \\ \langle b_2^2\rangle I & \langle b_2^2\rangle \end{pmatrix}\begin{pmatrix} a_1^{(j)} \\ a_2^{(j)} \end{pmatrix} = \nu^{(j)}\begin{pmatrix} a_1^{(j)} \\ a_2^{(j)} \end{pmatrix} \quad (52)$$

for the coefficients of the expansion (49). For standard parameter values, the leading EOF is found to be

$$E_\Phi^{(1)}(\phi) = -0.58F_1(\phi) + 0.81F_2(\phi). \quad (53)$$

This structure (the black curve in the upper panel of Fig. 4), strongly resembles the leading EOF for this case on a spherical domain (the gray curve in the upper panel of Fig. 4) as well as the observed annular mode (see Fig. 1), with oppositely signed anomalies in low and high latitudes and a zero crossing at ~55° (although the low-latitude extremum is too large, and the anomalies do not approach zero at the equatorward end of the domain). Note that the mixing of $F_1(\phi)$ and $F_2(\phi)$ in the EOFs occurs because these functions are not orthogonal, which itself is a consequence of the mass conservation constraint. The spatial correlation of $F_1(\phi)$ and $F_2(\phi)$ is weak, but sufficiently strong that the EOFs of $\Phi(\phi, t)$ are not in a one-to-one correspondence with the EOFs of $u(\phi, t)$.

The leading PC time series of $\Phi(\phi, t)$ is given by

$$\alpha_\Phi^{(1)}(t) = \int_{\phi_1}^{\phi_2} E_\Phi^{(1)}(\phi, t)\Phi(\phi, t)\, d\phi = (a_1^{(1)} + a_2^{(1)}\bar{I})b_1(t) + (a_2^{(1)} + a_1^{(1)}\bar{I})b_2(t). \quad (54)$$

It follows that the regression of $u(\phi, t)$ on $\alpha_\Phi^{(1)}(t)$ (normalized to unit variance) for standard parameter values is

$$\left\langle (u,(\phi, t) - \langle u(\phi)\rangle)\left(\frac{\alpha_\Phi^{(1)}}{\mathrm{std}(\alpha_\Phi^{(1)})}\right)\right\rangle \simeq -\frac{(a_1^{(1)} + a_2^{(1)}\bar{I})N_1\,\mathrm{var}(\alpha_u^{(1)})E_u^{(1)}(\phi) + (a_2^{(1)} + a_1^{(1)}\bar{I})N_2\,\mathrm{var}(\alpha_u^{(2)})E_u^{(2)}(\phi)}{\mathrm{std}(\alpha_\Phi^{(1)})}. \quad (55)$$

The regression pattern (the black curve in the lower panel of Fig. 4) projects onto both the first and second EOFs of zonal-mean zonal wind, with the consequence that the higher-latitude extremum is larger than the lower-latitude extremum. As was the case with the EOFs, this regression structure has a strong resemblance to that of the regression of the case of fluctuations in strength and position on a spherical domain (the gray curve in Fig. 4) and the regression of the observed annular mode on the zonal-mean zonal wind (Fig. 2).

We see from this example that domain size affects the EOF structure of geopotential in two ways. The first effect is on the variances of the time series $b_1(t)$ and $b_2(t)$ through the normalization factors N_1 and N_2. The second effect is on the orthogonality of $F_1(\phi)$ and $F_2(\phi)$, through the mass conservation constraint. If the size of the domain were to increase (equivalently, if the mean jet width were to shrink) sufficiently that $F_1(\phi)$ and $F_2(\phi)$ were orthogonal, then these patterns would be the EOFs. As the ratio N_2/N_1 increases without bound as the ratio of the domain width to σ_0 increases, for sufficiently large domains (or sufficiently small σ_0) $F_2(\phi)$ would necessarily be the leading EOF. For the standard parameters characteristic of the SH tropospheric eddy-driven jet, the EOF structure for the case of independent fluctuations in both strength and position is strongly affected by the fact that the observed jet is of hemispheric scale.

Furthermore, this calculation demonstrates that while individual fluctuations in strength, position, or width do not produce annular mode–like EOF structures, such structures do arise in the presence of simultaneous fluctuations in strength and position. The associated PC time series inextricably couples fluctuations in strength and position, such that the EOF mode cannot be associated with fluctuations in either jet degree of freedom individually.

5. Discussion and conclusions

This study has considered the EOF structure of zonal-mean geopotential $\Phi(\phi, t)$ in an idealized (but physically motivated) model of a midlatitude eddy-driven jet [in zonal-mean zonal wind $u(\phi, t)$], which fluctuates in strength, position, and width. The following results were obtained:

- The leading EOFs of observed austral summer (December–January) Southern Hemisphere zonal-mean zonal wind (the zonal index mode) and zonal-mean geopotential (the annular mode) are related, but distinct. The zonal index mode pattern and the regression pattern of the annular mode time series on zonal-mean zonal wind are both dipolar, but the regression pattern is considerably more asymmetric than the zonal index mode pattern. The correlation coefficient between the annular mode and zonal index is 0.90 ± 0.02: a high, but imperfect, correlation. The annular mode and the zonal index mode are not interchangeable.
- When the sphericity of the domain is accounted for in the translation from zonal-mean zonal wind to zonal-mean geopotential, the leading EOF of geopotential simulated by the idealized model is an excellent approximation to the observed annular mode when best-fit jet parameters obtained from observations are used. The spatial structures of the observed and simulated annular modes are very similar, as are the spatial structures of the regression of the annular mode time series on $u(\phi, t)$. Furthermore, the simulated annular mode and zonal index mode are not perfectly correlated: there is no one-to-one correspondence between EOF modes of $\Phi(\phi, t)$ and $u(\phi, t)$. In the model, as in the observations, the annular mode and the zonal index mode are related but distinct. The annular mode was found to be highly but not perfectly correlated with fluctuations in jet position. The annular mode cannot be associated with a unique jet degree of freedom.
- When the model includes fluctuations in only jet strength, position, or width individually, the simulated leading EOF mode of $\Phi(\phi, t)$ (on the spherical domain) is not in agreement with the observed annular mode. Unlike the dipole structure of the leading

EOF of zonal-mean zonal wind, which arises largely as a consequence of the symmetry of the zonal jet (Wittman et al. 2005; Monahan and Fyfe 2006), accurate simulation of the spatial structure of the annular mode requires fluctuations in at least jet strength and position be accounted for. Although the annular mode time series is not strongly correlated with jet strength or width, these jet degrees of freedom are needed for the accurate simulation of the annular mode.

- On a flat domain, the analytic results of Monahan and Fyfe (2006) can be extended to the EOFs and PC time series of zonal-mean geopotential by direct integration of the EOF expansions of zonal-mean zonal wind. This analysis makes it clear why one-to-one correspondence between individual EOFs of zonal-mean zonal wind and zonal-mean geopotential cannot be expected in general, and how the domain size and mass conservation constraint affect the ordering and structure of the zonal-mean geopotential EOFs. In particular, the hybridization of zonal-mean zonal wind EOFs in the EOFs of zonal-mean geopotential is shown to follow from the mathematical requirement that (by definition) EOF modes be orthogonal, as influenced by the physical constraint of mass conservation. Furthermore, the analytic results demonstrate that individual EOF modes of zonal-mean geopotential cannot be associated in general with individual jet degrees of freedom (strength, position, or width).

The results of Monahan and Fyfe (2006) and the present study reinforce the conclusion of Wittman et al. (2005) that the ubiquity of zonal index and annular mode structures over a broad range of atmospheric GCMs reflects the origin of these two structures in very generic aspects of variability in the eddy-driven jet. However, the relation of these patterns of variability to fluctuations in jet parameters is less clear: the annular mode time series has significant contributions from both variability in jet position and width. Similarly, it was shown in Monahan and Fyfe (2006) that variability in the zonal index time series will generally conflate fluctuations in jet position with those in jet strength and width. Furthermore, it was shown here that there is no general one-to-one relationship between individual EOF modes of the dynamically related fields of zonal-mean geopotential and zonal-mean zonal wind. An elegant discussion in general terms of why such an EOF mode–to–EOF mode connection cannot be expected for two physically related fields was given in Ambaum et al. (2001); the analysis given above demonstrates in detail how this connection fails in the particular case of extratropical zonal-mean zonal wind and zonal-mean geopotential.

This study considers variability in the austral summertime SH extratropical circulation, which is characterized by a single, eddy-driven jet. In other seasons, the kinematics of extratropical variability are complicated by the presence of both subtropical and eddy-driven jets, the fluctuations of which are not independent (Lee and Kim 2003). The present study has focused on the relatively simple case primarily because the Gaussian jet fitting procedure (described in Monahan and Fyfe 2006) works best when the observations contain only a single jet. An analysis of the zonal index mode and annular mode in the SH austral wintertime (not shown) is in qualitative agreement with the results presented in this study. This fact and the generality of the arguments presented above suggest that the main conclusions of this study are not affected by the presence of more than one fluctuating jet. However, because the kinematics of the extratropical circulation will certainly be different in detail when more than one jet is present, an interesting direction of future research would repeat the analysis of this study with a model, including both eddy-driven and subtropical jets.

The intent of the present study is not to suggest that either of the zonal index mode or the annular mode characterizations of extratropical atmospheric variability is superior to the other. Empirical orthogonal function modes are statistical constructs, and in this sense both the annular mode and the zonal index mode are equally valid. What this study does show is that these commonly used characterizations of the kinematics of the extratropical flow do not have simple relationships to the structure of the eddy-driven jet, or to each other. Monahan and Fyfe (2006) demonstrated the need to exercise caution in interpreting individual EOF modes in terms of individual jet degrees of freedom; the present study further demonstrates the need for caution when comparing EOF modes of dynamically related fields on a one-to-one basis.

Because the model used in this study is idealized, it does not (and cannot be expected to) provide an exact characterization of the observed kinematics of the zonal-mean zonal jet. In particular, the correlation between the annular mode and zonal index mode time series is higher in observations than in the model; as well, the observed zonal index mode is characterized by an asymmetry in the magnitudes of the lobes of the dipole not present in the modeled zonal index structure. However, when best-fit jet parameters are used, the idealized fluctuating jet model considered in this study provides a good first-order characterization of the SH summertime zonal index mode, the annular mode,

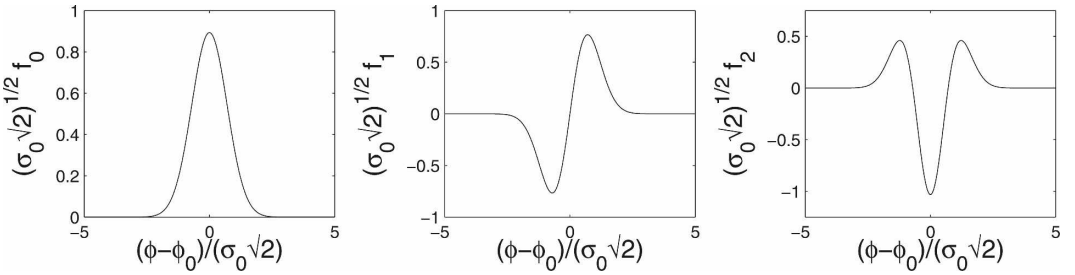

FIG. A1. Plots of the basis functions $f_0(\phi)$, $f_1(\phi)$, and $f_2(\phi)$ [Eq. (A5)], rescaled to be of unit norm.

and their interrelation, and therefore serves as a useful null hypothesis for explaining the observed EOF structures of the zonal-mean circulation, which play such a fundamental role in the discussions of extratropical atmospheric low-frequency variability (e.g., Thompson et al. 2002). The underlying physical processes producing the jet and its variability are not considered by this idealized model, and are themselves the subjects of active research (e.g., Robinson 1996; Feldstein and Lee 1998; DeWeaver and Nigam 2000; Lorenz and Hartmann 2001; Codron 2005). Rather, the results of this study reinforce the centrality of the fluctuating eddy-driven jet to the zonal-mean low-frequency variability of the extratropical atmosphere and provide guidance for interpreting the observed statistical structures in terms of underlying physical degrees of freedom.

Acknowledgments. The authors thank Alexey Kaplan, Lorenzo Polvani, and Ed Gerber for helpful discussions, and William Merryfield and Ken Denman for helpful comments on a draft of this manuscript. This manuscript was also significantly improved by the helpful comments of three anonymous reviewers. Adam Monahan acknowledges support from the Natural Sciences and Engineering Research Council of Canada and from the Canadian Institute for Advanced Research Earth System Evolution Program.

APPENDIX

EOFs and Basis Functions

The EOFs $E_Z^{(j)}(\phi)$ of a space–time field $Z(\phi, t)$ are the eigenvectors of the covariance function

$$C_{ZZ}(\phi', \phi'') = \langle Z(\phi')Z(\phi'')\rangle - \langle Z(\phi')\rangle\langle Z(\phi'')\rangle \quad \text{(A1)}$$

(where angle brackets denote ensemble or time averaging), obtained as solutions of the integral equation

$$\int_{\phi_1}^{\phi_2} C_{ZZ}(\phi', \phi'')E_Z^{(j)}(\phi'')\, d\phi'' = \mu_Z^{(j)}E_Z^{(j)}(\phi'). \quad \text{(A2)}$$

The PC time series $\alpha_Z^{(j)}(t)$ are obtained through projection of $Z(\phi, t)$ on to $E_Z^{(j)}(\phi)$:

$$\alpha_Z^{(j)}(t) = \int_{\phi_1}^{\phi_2} Z(\phi, t)E_Z^{(j)}(\phi)\, d\phi. \quad \text{(A3)}$$

The EOFs form an orthonormal basis, so the field $Z(\phi)$ has the EOF expansion

$$Z(\phi, t) = \sum_{j=1}^{\infty} \alpha_Z^{(j)}(t)E_Z^{(j)}(\phi). \quad \text{(A4)}$$

Together, the corresponding EOF spatial pattern and PC time series are denoted an EOF mode.

Monahan and Fyfe (2006) demonstrated the relevance to the covariance structure of the fluctuating Gaussian jet of the basis functions

$$f_n(\phi) = \mathcal{N}_n H_n\left(\frac{\phi - \phi_0}{\sqrt{2}\sigma_0}\right)\exp\left(-\frac{(\phi - \phi_0)^2}{2\sigma_0^2}\right), \quad \text{(A5)}$$

where $H_n(x)$ are the Hermite polynomials and the coefficients $\mathcal{N}_n$ are defined by the normalization constraint

$$\int_{\phi_1}^{\phi_2} f_n^2(\phi)\, d\phi = 1. \quad \text{(A6)}$$

As long as the width of the analysis domain around ϕ_0 is greater than a few multiples of σ_0, this integral will be essentially independent of the domain size with value

$$\mathcal{N}_n = [\sigma_0 2^n \Gamma(n + 1/2)]^{-1/2}. \quad \text{(A7)}$$

In particular, the functions $f_n(\phi)$ are square integrable on $(-\infty, \infty)$. Plots of the functions $f_i(\phi)$ for $i = 0, 1, 2$ (respectively, monopole, dipole, and tripole structures) are given in Fig. A1.

Using the recursion relationship for Hermite polynomials,

$$H_n(x) = 2xH_{n-1}(x) - H'_{n-1}(x) \quad \text{(A8)}$$

(e.g., Gradshteyn and Ryzhik 2000), it is easy to show that the functions $f_n(\phi)$ satisfy the recursion relationship

$$\frac{df_n}{d\phi} = -\frac{1}{\sigma_0}\left(n + \frac{1}{2}\right)^{1/2} f_{n+1}(\phi)(n = 0, 1, 2, \ldots), \quad \text{(A9)}$$

or, equivalently,

$$\int f_n(\phi')\, d\phi' = -\sigma_0\left(n - \frac{1}{2}\right)^{-1/2} f_{n-1}(\phi)(n = 1, 2, 3, \ldots). \quad \text{(A10)}$$

While differentiation does not introduce any new basis functions, integration does for $n = 0$:

$$\int f_0(\phi)\, d\phi = \left(\frac{2\sigma_0}{\sqrt{\pi}}\right)^{1/2} \mathrm{erf}\left(\frac{\phi - \phi_0}{\sqrt{2}\sigma_0}\right). \quad \text{(A11)}$$

Note that unlike the functions $f_n(\phi)$ $(n = 0, 1, 2, \ldots)$, the error function $\mathrm{erf}[(\phi - \phi_0)/\sqrt{2}\sigma_0]$ is not square integrable on $(-\infty, \infty)$ and that

$$\int_{\phi_1}^{\phi_2} \mathrm{erf}^2\left(\frac{\phi - \phi_0}{\sqrt{2}\sigma_0}\right) d\phi = A(\phi_1, \phi_2)(\phi_2 - \phi_1), \quad \text{(A12)}$$

where $A(\phi_1, \phi_2)$ is $O(1)$. The normalization of this function thus depends on the size of the domain.

REFERENCES

Ambaum, M. H., B. J. Hoskins, and D. B. Stephenson, 2001: Arctic Oscillation or North Atlantic Oscillation? *J. Climate,* **14,** 3495–3507.

Baldwin, M., 2001: Annular modes in global daily surface pressure. *Geophys. Res. Lett.,* **28,** 4115–4118.

Cash, B., P. Kushner, and G. Vallis, 2002: The structure and composition of the annular modes in an aquaplanet general circulation model. *J. Atmos. Sci.,* **59,** 3399–3414.

Codron, F., 2005: Relation between annular modes and the mean state: Southern Hemisphere summer. *J. Climate,* **18,** 320–330.

DeWeaver, E., and S. Nigam, 2000: Do stationary waves drive the zonal-mean jet anomalies of the northern winter? *J. Climate,* **13,** 2160–2176.

Feldstein, S., and S. Lee, 1998: Is the atmospheric zonal index driven by an eddy feedback? *J. Atmos. Sci.,* **55,** 3077–3086.

Fyfe, J. C., 2003: Separating extratropical zonal wind variability and mean change. *J. Climate,* **16,** 863–874.

——, and D. J. Lorenz, 2005: Characterizing zonal wind variability: Lessons from a simple GCM. *J. Climate,* **18,** 3400–3404.

Gerber, E. P., and G. K. Vallis, 2005: A stochastic model for the spatial structure of annular patterns of variability and the North Atlantic Oscillation. *J. Climate,* **18,** 2102–2118.

Gradshteyn, I., and I. Ryzhik, 2000: *Table of Integrals, Series, and Products.* 6th ed. Academic Press, 1163 pp.

Kushner, P. J., and G. Lee, 2007: Resolving the regional signature of the annular modes. *J. Climate,* **20,** 2840–2852.

Lee, S., and H.-K. Kim, 2003: The dynamical relationship between subtropical and eddy-driven jets. *J. Atmos. Sci.,* **60,** 1490–1503.

Limpasuvan, V., and D. L. Hartmann, 2000: Wave-maintained annular modes of climate variability. *J. Climate,* **13,** 4414–4429.

Lorenz, D. J., and D. L. Hartmann, 2001: Eddy-zonal flow feedback in the Southern Hemisphere. *J. Atmos. Sci.,* **58,** 3312–3327.

Monahan, A. H., and J. C. Fyfe, 2006: On the nature of zonal jet EOFs. *J. Climate,* **19,** 6409–6424.

Robinson, W., 1996: Does eddy feedback sustain variability in the zonal index? *J. Atmos. Sci.,* **53,** 3556–3569.

Thompson, D. W., and J. M. Wallace, 1998: The Arctic Oscillation signature in the wintertime geopotential height and temperature fields. *Geophys. Res. Lett.,* **25,** 1297–1300.

——, and ——, 2000: Annular modes in the extratropical circulation. Part I: Month-to-month variability. *J. Climate,* **13,** 1000–1016.

——, S. Lee, and M. Baldwin, 2002: Atmospheric processes governing the Northern Hemisphere Annular Mode/North Atlantic Oscillation. *The North Atlantic Oscillation: Climatic Significance and Environmental Impact, Geophys. Monogr.,* Vol. 134, Amer. Geophys. Union, 81–112.

Vallis, G. K., E. P. Gerber, P. J. Kushner, and B. A. Cash, 2004: A mechanism and simple dynamical model of the North Atlantic Oscillation and annular modes. *J. Atmos. Sci.,* **61,** 264–280.

Wallace, J. M., 2000: North Atlantic Oscillation/Annular Mode: Two paradigms–one phenomenon. *Quart. J. Roy. Meteor. Soc.,* **126,** 791–806.

Wittman, M. A., A. J. Charlton, and L. M. Polvani, 2005: On the meridional structure of annular modes. *J. Climate,* **18,** 2119–2122.